

Histogram of Gradient Orientations of Signal Plots applied to P300 Detection

Rodrigo Ramele^{1,*}, Ana Julia Villar¹ and Juan Miguel Santos¹

¹*Centro de Inteligencia Computacional, Computer Engineering Department,
Instituto Tecnológico de Buenos Aires, Buenos Aires, Argentina*

Correspondence*:

Rodrigo Ramele, C1437FBH Lavarden 315, Ciudad Autónoma de Buenos Aires,
Argentina
rramele@itba.edu.ar

2 ABSTRACT

3 Word Count: 4952

4 The analysis of Electroencephalographic (EEG) signals is of ulterior importance ~~for decoding~~
5 ~~patterns that could improve the implementation of Brain Computer Interfaces (BCI). These~~
6 ~~systems are meant to provide alternative to aid in the diagnosis of mental disease and to~~
7 ~~increase our understanding of the brain. Traditionally, clinical EEG has been analyzed in terms~~
8 ~~of temporal waveforms, looking at rhythms in spontaneous activity, subjectively identifying~~
9 ~~troughs and peaks in Event-Related Potentials (ERP), or by studying graphoelements in~~
10 ~~pathological sleep stages. Additionally, the discipline of Brain Computer Interfaces requires new~~
11 ~~methods to decode patterns from non-invasive EEG signals. This field is developing alternative~~
12 ~~communication pathways to transmit volitional information ~~which~~ from the Central Nervous~~
13 ~~System. The technology~~ could potentially enhance the quality of life of patients affected by
14 neurodegenerative disorders and other mental illness. ~~Of particular interests are those which~~
15 ~~are based on the recognition of Event-Related Potentials (ERP) because they can be elicited by~~
16 ~~external stimuli and used to implement spellers, to control external devices or even avatars in~~
17 ~~virtual reality environments.~~ This work mimics what electroencephalographers have been doing
18 clinically, visually inspecting and categorizing phenomena within the EEG by the extraction of
19 features from images of signal plots. ~~It also, but~~ aims to provide a ~~new objective~~ framework to
20 analyze, characterize and classify EEG ~~signals, with a focus on the~~ signal waveforms. These
21 ~~features are constructed based on the calculation of histograms of the oriented gradients from~~
22 ~~pixels around the signal plot. The feasibility of the method is outlined by detecting the~~ P300, an
23 ~~ERP elicited by the oddball paradigm of rare events, and implementing an offline P300-based~~
24 ~~BCI Speller.~~ The validity of the ~~method proposal~~ is shown by offline processing a public dataset
25 of Amyotrophic Lateral Sclerosis (ALS) patients and an own dataset of healthy subjects.

26 **Keywords:** electroencephalography, histogram of gradient orientations, brain-computer interfaces, P300, SIFT, amyotrophic lateral
27 sclerosis, naive-bayes near neighbours, waveforms

1 INTRODUCTION

28 Although recent advances in neuroimaging techniques, particularly radio-nuclear and radiological
29 scanning methods (?), have diminished the prospects of the traditional Electroencephalography (EEG),

30 the advent and development of digitized devices has impelled for a revamping of this hundred years old
31 technology. Their versatility, ease of use, temporal resolution, ease of development and production, and
32 its proliferation as consumer devices, are pushing EEG to become the de-facto non invasive portable or
33 ambulatory method to access and harness brain information (?).

34 A key contribution to this expansion has been the field of Brain Computer Interfaces (BCI) (?) which is
35 the pursuit of the development of a new channel of communication particularly aimed to persons affected
36 by neurodegenerative diseases.

37 One noteworthy aspect of this novel communication channel is the ability to transmit information from
38 the Central Nervous System (CNS) to a computer device and from there use that information to control a
39 wheelchair (?), as input to a speller application (?), in a Virtual Reality environment (?) or as aiding tool
40 in a rehabilitation procedure (?). The holly grail of BCI is to implement a new complete and alternative
41 pathway to restore lost locomotion (?).

42 EEG signals are remarkably complex and have been characterized as a multichannel non-stationary
43 stochastic process. Additionally, they have high variability between different subjects and even between
44 different moments for the same subject, requiring adaptive and co-adaptive calibration and learning
45 procedures (?). Hence, this imposes an outstanding challenge that is necessary to overcome in order to
46 extract information from raw EEG signals.

47 BCI has gained mainstream public awareness with worldwide challenge competitions like Cybathlon (??)
48 and even been broadcasted during the inauguration ceremony of the 2014 Soccer World Cup. New
49 developments have overcome the out-of-the-lab high-bar and they are starting to be used in real world
50 environments (??). However, they still lack the necessary robustness, and its performance is well behind
51 any other method of human computer interaction, including any kind of detection of residual muscular
52 movement (?).

53 A few works have explored the idea of exploiting the signal waveform to analyze the EEG signal. In (?)
54 an approach based on Slope Horizontal Chain Code is presented, whereas in (?) a similar procedure
55 was implemented based on Mathematical Morphological Analysis. The seminal work of Bandt-Pompe
56 Permutation Entropy (?) also explores succinctly this idea as a basis to establish the time series ordinal
57 patterns. In the article (?), the authors introduce a method for classification of rhythmic EEG events like
58 Visual Occipital Alpha Waves and Motor Imagery Rolandic Central μ Rhythms using the [histogram of](#)
59 [gradient orientations](#) [Histogram of Gradient Orientations](#) of signal plots. Inspired in that work, we propose
60 a novel application of the developed method to classify and describe transient events, particularly the P300
61 Event Related Potential. The proposed approach is based on the waveform analysis of the shape of the EEG
62 signal, ~~but using histogram of gradient orientations~~. The signal is drawn on a bidimensional image plot,
63 vector gradients of pixels around the plot are obtained, and with them, the histogram of their orientations
64 is calculated. This histogram is a direct representation of the waveform of the signal. The method is built
65 by mimicking what regularly electroencephalographers have been performing for almost a century as it is
66 described in (?): visually inspecting raw signal plots.

67 This paper reports a method to, (1) describe a procedure to capture the shape of a waveform of an ERP
68 component, the P300, using histograms of gradient orientations extracted from images of signal plots, and
69 (2) outline the way in which this procedure can be used to implement an ~~offline P300-based~~ [P300-Based](#)
70 BCI Speller application. Its validity is verified by offline processing two datasets, one of data from ALS
71 patients and another one from data of healthy subjects.

This article unfolds as follows: Section 2.1 is dedicated to explain the Feature Extraction method based on Histogram of Gradient Orientations of the Signal Plot: Section 2.1.1 shows the preprocessing pipeline, Section 2.1.2 describes the image generation of the signal plot, Section 2.1.3 presents the feature extraction procedure while Section 2.1.4 introduces the Speller Matrix Letter Identification procedure. In Section 2.2, the experimental protocol is expounded. Section 3 shows the results of applying the proposed technique. In the final Section 4 we expose our remarks, conclusions and future work.

2 MATERIALS AND METHODS

The P300 (??) is a positive deflection of the EEG signal which occurs around 300 ms after the onset of a rare and deviant stimulus that the subject is expected to attend. It is produced under the oddball paradigm (?) and it is consistent across different subjects. It has a lower amplitude ($\pm 5\mu V$) compared to basal EEG activity, reaching a Signal to Noise Ratio (SNR) of around -15 db estimated based on the amplitude of the P300 response signal divided by the standard deviation of the background EEG activity (?). This signal can be used to implement a speller application by means of a Speller Matrix (?). This matrix is composed of 6 rows and 6 columns of numbers and letters. The subject can focus on one character of the matrix. Figure 1 shows an example of the Speller Matrix used in the OpenVibe open source software (?), where the flashes of rows and columns provide the deviant stimulus required to elicit this physiological response. Each time a row or a column that contains the desired letter flashes, the corresponding synchronized EEG signal should also contain the P300 signature and by detecting it, the selected letter can be identified.

2.1 Feature Extraction from Signal Plots

In this section, the signal preprocessing, the method for generating images from signal plots, the feature extraction procedure and the Speller Matrix identification are described. Figure 2 shows a scheme of the entire process.

2.1.1 Preprocessing Pipeline

The data obtained by the capturing device is digitalized and a multichannel EEG signal is constructed.

The 6 rows and 6 columns of the Speller Matrix are intensified providing the visual stimulus. The number of a row or column is a location. A sequence of twelve randomly permuted locations l conform an intensification sequence. The whole set of twelve intensifications is repeated k_a times.

• **Signal Enhancement:** This stage consists of the enhancement of the SNR of the P300 pattern above the level of basal EEG. The pipeline starts by applying a notch filter to the raw digital signal, a 4th degree 10 Hz lowpass Butterworth filter and finally a decimation with a Finite Impulse Response (FIR) filter of order 30 from the original sampling frequency down to 16 Hz (?).

• **Artifact Removal:** For every complete sequence of 12 intensifications of 6 rows and 6 columns, a basic artifact elimination procedure is implemented by removing the entire sequence when any signal deviates above/below $\pm 70\mu V$.

• **Segmentation:** For each of the 12 intensifications of one intensification sequence, a segment S_i^l of a window of t_{max} seconds of the multichannel signal is extracted, starting from the stimulus onset, corresponding to each row/column intensification l and to the intensification sequence i . As intensifications are permuted in a random order, the segments are rearranged corresponding to row flickering, labeled 1-6, whereas those corresponding to column flickering are labeled 7-12. Two of

110 these segments should contain the P300 ERP signature time-locked to the flashing stimulus, one for
 111 the row, and one for the column.

112 • **Signal Averaging:** The P300 ERP is deeply buried under basal EEG so the standard approach to
 113 identify it is by point-to-point averaging the time-locked stacked signal segments. Hence the values
 114 which are not related to, and not time-locked to the onset of the stimulus are canceled out (?).

115 This last step determines the operation of any P300 Speller. In order to obtain an improved signal
 116 in terms of its SNR, repetitions of the sequence of row/column intensification are necessary. And,
 117 at the same time, as long as more repetitions are needed, the ability to transfer information faster is
 118 diminished, so there is a trade-off that must be acutely determined.

119 The procedure to obtain the point-to-point averaged signal goes as follows:

120 1. Highlight randomly the rows and columns from the matrix. There is one row and one column that
 121 should match the letter selected by the subject.

122 2. Repeat step 1 k_a times, obtaining the $1 \leq l \leq 12$ segments $S_1^l(n, c), \dots, S_{k_a}^l(n, c)$, of the EEG
 123 signal where the variables $1 \leq n \leq n_{max}$ and $1 \leq c \leq C$ correspond to sample points and channel,
 124 respectively. The parameter C is the number of available EEG channels whereas $n_{max} = F_s t_{max}$
 125 is the segment length and F_s is the sampling frequency. The parameter k_a is the number of
 126 repetitions of intensifications and it is an input parameter of the algorithm.

127 3. Compute the Ensemble Average by

$$x^l(n, c) = \frac{1}{k_a} \sum_{i=1}^{k_a} S_i^l(n, c) \quad (1)$$

128 for $1 \leq n \leq n_{max}$ and for the channels $1 \leq c \leq C$. This provide an averaged signal $x^l(n, c)$ for
 129 the twelve locations $1 \leq l \leq 12$.

130 2.1.2 Signal Plotting

131 Averaged signal segments are standardized and scaled for $1 \leq n \leq n_{max}$ and $1 \leq c \leq C$ by

$$\tilde{x}^l(n, c) = \left[\gamma \frac{(x^l(n, c) - \bar{x}^l(c))}{\hat{\sigma}^l(c)} \right] \quad (2)$$

where $\gamma > 0$ is an input parameter of the algorithm and it is related to the image scale. In addition, $x^l(n, c)$ is the point-to-point averaged multichannel EEG signal for the sample point n and for channel c . Lastly,

$$\bar{x}^l(c) = \frac{1}{n_{max}} \sum_{n=1}^{n_{max}} x^l(n, c)$$

and

$$\hat{\sigma}^l(c) = \left(\frac{1}{n_{max} - 1} \sum_{n=1}^{n_{max}} (x^l(n, c) - \bar{x}^l(c))^2 \right)^{\frac{1}{2}}$$

132 are the mean and estimated standard deviation of $x^l(n, c)$, $1 \leq n \leq n_{max}$, for each channel c .

133 Consequently, ~~for a pixel (z_1, z_2) , the a binary~~ image $I^{(l,c)}$ is constructed according to

$$I^{(l,c)}(z_1, z_2) = \begin{cases} 255 & \text{if } z_1 = \gamma n; z_2 = \tilde{x}^l(n, c) + z^l(c) \\ 0 & \text{otherwise} \end{cases} \quad (3)$$

134 where with 255 being white and representing the signal's value location and 0 for black which is the
 135 background contrast, conforming a black-and-white plot of the signal. Pixel arguments $(z_1, z_2) \in \mathbb{N} \times \mathbb{N}$
 136 iterate over the width (based on the length of the signal segment) and height (based on the peak-to-peak
 137 amplitude) of the newly created image with $1 \leq n \leq n_{max}$ and $1 \leq c \leq C$. The value $z^l(c)$ is the image
 138 vertical position where the signal's zero value has to be situated in order to fit the entire signal within the
 139 image for each channel c:

$$z^l(c) = \left\lfloor \frac{\max_n \tilde{x}^l(n, c) - \min_n \tilde{x}^l(n, c)}{2} \right\rfloor - \left\lfloor \frac{\max_n \tilde{x}^l(n, c) + \min_n \tilde{x}^l(n, c)}{2} \right\rfloor \quad (4)$$

140 where the minimization and maximization are carried out for n varying between $1 \leq n \leq n_{max}$, and $\lfloor \cdot \rfloor$
 141 denote the rounding to the smaller nearest integer of the number.

142 In order to complete the plot $I^{(l,c)}$ from the pixels, the Bresenham (??) algorithm is used to interpolate
 143 straight lines between each pair of consecutive pixels.

144 2.1.3 Feature Extraction: Histogram of Gradient Orientations

145 For each generated image $I^{(l,c)}$, a keypoint \mathbf{p}_k is placed on a pixel (x_{p_k}, y_{p_k}) over the image plot and a
 146 window around the keypoint is considered. A local image patch of size $X_p \times X_p$ pixels is constructed by
 147 dividing the window in 16 blocks of size $3s$ each one, where s is the scale of the local patch and it is an
 148 input parameter of the algorithm. It is arranged in a 4×4 grid and the pixel \mathbf{p}_k is the patch center, thus
 149 $X_p = 12s$ pixels.

150 A local representation of the signal shape within the patch can be described by obtaining the gradient
 151 orientations on each of the 16 blocks $B_{i,j}$ with $0 \leq i, j \leq 3$ and creating a histogram of gradients. This
 152 technique is based on Lowe's SIFT (?) method, and it is biomimetically inspired in how the visual cortex
 153 detects shapes by analyzing orientations (?). In order to calculate the histogram, the interval $[0, 360]$ of
 154 possible angles is divided in 8 bins, each one of 45 degrees.

155 Hence, for each spatial bin $0 \leq i, j \leq 3$, corresponding to the indexes of each block $B_{i,j}$, the orientations
 156 are accumulated in a 3-dimensional histogram h through the following equation:

$$h(\theta, i, j) = 3s \sum_{\mathbf{p} \in I^{(l,c)}} w_{ang}(\angle J(\mathbf{p}) - \theta) w_{ij} \left(\frac{\mathbf{p} - \mathbf{p}_k}{3s} \right) |J(\mathbf{p})| \quad (5)$$

157 where \mathbf{p} is a pixel from the image $I^{(l,c)}$, θ is the angle bin with $\theta \in \{0, 45, 90, 135, 180, 225, 270, 315\}$,
 158 $|J(\mathbf{p})|$ is the norm of the gradient vector in the pixel \mathbf{p} and it is computed using finite differences and $\angle J(\mathbf{p})$
 159 is the angle of the gradient vector. The scalar $w_{ang}(\cdot)$ and vector $w_{ij}(\cdot)$ functions are linear interpolations
 160 used by ? and ? to provide a weighting contribution to eight adjacent bins. They are calculated as

$$w_{ij}(\mathbf{v}) = w(v_x - x_i)w(v_y - y_j) \quad (6)$$

161 with $0 \leq i, j \leq 3$ and

$$w_{\text{ang}}(\alpha) = \sum_{r=-1}^1 w\left(\frac{8\alpha}{2\pi} + 8r\right) \quad (7)$$

162 where x_i and y_i are the spatial bin centers located in $x_i, y_j \in \{-\frac{3}{2}, -\frac{1}{2}, \frac{1}{2}, \frac{3}{2}\}$, $\mathbf{v} = (v_x, v_y)$ is a vector
 163 variable and α a scalar variable. On the other hand, r is an integer that can vary freely between $[-1, 1]$
 164 which allows the argument α to be unconstrained in terms of its values in radians. The interpolating
 165 function $w(\cdot)$ is defined as $w(z) = \max(0, |z| - 1)$.

166 These binning functions conform a trilinear interpolation that has a combined effect of sharing the
 167 contribution of each oriented gradient between their eight adjacent bins in a tridimensional cube in the
 168 histogram space, and zero everywhere else.

169 Lastly, the fixed value of 3 is a magnification factor which corresponds to the number of pixels per each
 170 block when $s = 1$. As the patch has 16 blocks and 8 bin angles are considered, for each location l and
 171 channel c a feature called *descriptor* $\mathbf{d}^{(l,c)}$ of 128 dimension is obtained.

172 Figure 3 shows an example of a patch and a scheme of the histogram computation. In (A) a plot of the
 173 signal and the patch centered around the keypoint is shown. In (B) the possible orientations on each patch
 174 are illustrated. Only the upper-left four blocks are visible. The first eight orientations of the first block, are
 175 labeled from 1 to 8 clockwise. The orientations of the second block $B_{1,2}$ are labeled from 9 to 16. This
 176 labeling continues left-to-right, up-down until the eight orientations for all the sixteen blocks are assigned.
 177 They form the corresponding descriptor \mathbf{d} of 128 coordinates. Finally, in (C) an enlarged image plot is
 178 shown where the oriented gradient vector for each pixel can be seen.

179 2.1.4 Speller Matrix letter Identification

180 2.1.4.1 P300 ERP Extraction

181 Segments corresponding to row flickering are labeled 1-6, whereas those corresponding to column
 182 flickering are labeled 7-12. The extraction process has the following steps:

- 183 • **Step A:** First highlight rows and columns from the matrix in a random permutation order and obtain
 184 the Ensemble Average as detailed in steps 1, 2 and 3 in Section 2.1.1.
- 185 • **Step B:** Plot the signals $\tilde{x}^l(n, c)$, $1 \leq n \leq n_{\text{max}}$, $1 \leq c \leq C$, according Section 2.1.2 in order to
 186 generate the images $I^{(l,c)}$ for rows and columns $1 \leq l \leq 12$.
- 187 • **Step C:** Obtain the descriptors $\mathbf{d}^{(l,c)}$ for rows and columns from $I^{(l,c)}$ in accordance to the method
 188 described in Section 2.1.3.

189 2.1.4.2 Calibration

190 A trial, as defined by the BCI2000 platform (?), is every attempt to select just one letter from the speller.
 191 A set of trials is used for calibration and once the calibration is complete it can be used to identify new
 192 letters from new trials.

193 During the calibration phase, two descriptors $\mathbf{d}^{(l,c)}$ are extracted for each available channel, corresponding
 194 to the locations l of a selection of one previously instructed letter from the set of calibration trials. These
 195 descriptors are the P300 templates, grouped together in a template set called T^c . The set is constructed
 196 using the steps described in Section 2.1.1 and the steps A, B and C of the P300 ERP extraction process.

197 Additionally, the best performing channel, bpc is identified based on the the channel where the best
 198 Character Recognition Rate is obtained.

199 **2.1.4.3 Letter identification**

200 In order to identify the selected letter, the template set T^{bpc} is used as a database. Thus, new descriptors
 201 are computed and they are compared against the descriptors belonging to the calibration template set T^{bpc} .

202 • **Step D:** Match to the calibration template T^{bpc} by computing

$$\hat{row} = \arg \min_{l \in \{1, \dots, 6\}} \sum_{q \in N_T(\mathbf{d}^{(l,bpc)})} \left\| q - \mathbf{d}^{(l,bpc)} \right\|^2 \quad (8)$$

203 and

$$\hat{col} = \arg \min_{l \in \{7, \dots, 12\}} \sum_{q \in N_T(\mathbf{d}^{(l,bpc)})} \left\| q - \mathbf{d}^{(l,bpc)} \right\|^2 \quad (9)$$

204 where $N_T(\mathbf{d}^{(l,bpc)})$ is defined as $N_T(\mathbf{d}^{(l,bpc)}) = \{\mathbf{d} \in T^{bpc} / \mathbf{d}$ is the k-nearest neighbor of $\mathbf{d}^{(l,bpc)}$ } for
 205 the best performing channel. This set is obtained by sorting all the elements in T^{bpc} based on distances
 206 between them and $\mathbf{d}^{(l,bpc)}$, choosing the k with smaller values, with k a parameter of the algorithm.
 207 This procedure is based on the k-NBNN algorithm (?).

208 By computing the aforementioned equations, the letter of the matrix can be determined from the intersection
 209 of the row \hat{row} and column \hat{col} . Figure 2 shows a scheme of this process.

210 **2.2 Experimental Protocol**

211 To verify the validity of the proposed framework and method, the public dataset 008-2014 (?) published
 212 on the BNCI-Horizon website (?) by IRCCS Fondazione Santa Lucia, is used. Additionally, an own dataset
 213 with the same experimental conditions is generated. Both of them are utilized to perform an offline BCI
 214 Simulation to decode the spelled words from the provided signals.

215 The algorithm is implemented using VLFeat (?) Computer Vision libraries on MATLAB V2014a
 216 (Mathworks Inc., Natick, MA, USA). Furthermore, in order to enhance the impact of our paper and for a
 217 sake of reproducibility, the code of the algorithm has been made available at: <https://bitbucket.org/itba/hist>.

218 In the following sections the characteristics of the datasets and parameters of the identification algorithm
 219 are described.

220 **2.2.1 P300 ALS Public Dataset**

221 The experimental protocol used to generate this dataset is explained in (?) but can be summarized as
 222 follows: 8 subjects with confirmed diagnoses but on different stages of ALS disease, were recruited and
 223 accepted to perform the experiments. The Visual P300 detection task designed for this experiment consisted
 224 of spelling 7 words of 5 letters each, using the traditional P300 Speller Matrix (?). The flashing of rows
 225 and columns provide the deviant stimulus required to elicit this physiological response. The first 3 words
 226 are used for calibration and the remaining 4 words, for testing with visual feedback. A trial is every attempt
 227 to select a letter from the speller. It is composed of signal segments corresponding to $k_a = 10$ repetitions
 228 of flashes of 6 rows and $k_a = 10$ repetitions of flashes of 6 columns of the matrix, yielding 120 repetitions.
 229 Flashing of a row or a column is performed for 0.125 s, following by a resting period (i.e. inter-stimulus

230 interval) of the same length. After 120 repetitions an inter-trial pause is included before resuming with the
231 following letter.

232 The recorded dataset was sampled at 256 Hz and it consisted of a scalp multichannel EEG signal for
233 electrode channels Fz, Cz, Pz, Oz, P3, P4, PO7 and PO8, identified according to the 10-20 International
234 System, for each one of the 8 subjects. The recording device was a research-oriented digital EEG device
235 (g.Mobilab, g.Tec, Austria) and the data acquisition and stimuli delivery were handled by the BCI2000
236 open source software (?).

237 In order to assess and verify the identification of the P300 response, subjects are instructed to perform a
238 copy-spelling task. They have to fix their attention to successive letters for copying a previously determined
239 set of words, in contrast to a free-running operation of the speller where each user decides on its own what
240 letter to choose.

241 2.2.2 P300 for healthy subjects

242 We replicate the same experiment on healthy subjects using a wireless digital EEG device (g.Nautilus,
243 g.Tec, Austria). The experimental conditions are the same as those used for the previous dataset, as detailed
244 in section 2.2.1. The produced dataset is available in a public online repository (?).

245 Participants are recruited voluntarily and the experiment is conducted anonymously in accordance with
246 the Declaration of Helsinki published by the World Health Organization. No monetary compensation
247 is handed out and all participants agree and sign a written informed consent. This study is approved
248 by the *Departamento de Investigación y Doctorado, Instituto Tecnológico de Buenos Aires (ITBA)*. All
249 healthy subjects have normal or corrected-to-normal vision and no history of neurological disorders. The
250 experiment is performed with 8 subjects, 6 males, 2 females, 6 right-handed, 2 left-handed, average age
251 29.00 years, standard deviation 11.56 years, range 20-56 years.

252 EEG data is collected in a single recording session. Participants are seated in a comfortable chair, with
253 their vision aligned to a computer screen located one meter in front of them. The handling and processing
254 of the data and stimuli is conducted by the OpenVibe platform (?).

255 Gel-based active electrodes (g.LADYbird, g.Tec, Austria) are used on the same positions Fz, Cz, Pz,
256 Oz, P3,P4, PO7 and PO8. Reference is set to the right ear lobe and ground is preset as the AFz position.
257 Sampling frequency is slightly different, and is set to 250 Hz, which is the closest possible to the one used
258 with the other dataset.

259 2.2.3 Parameters

260 The patch size is $X_P = 12s \times 12s$ pixels, where s is the scale of the local patch and it is an input parameter
261 of the algorithm. The P300 event can have a span of 400 ms and its amplitude can reach $10\mu V$ (?). Hence
262 it is necessary to utilize a signal segment of size $t_{max} = 1$ second and a size patch X_P that could capture
263 an entire transient event. With this purpose in consideration, the s value election is essential.

264 We propose the Equations 10 and 11 to compute the scale value in horizontal and vertical directions,
265 respectively.

$$s_x = \frac{\gamma \lambda F_s}{12} \quad (10)$$

$$s_y = \frac{\gamma \Delta \mu V}{12} \quad (11)$$

where λ is the length in seconds covered by the patch, F_s is the sampling frequency of the EEG signal (downsampled to 16 Hz) and $\Delta\mu V$ corresponds to the amplitude in microvolts that can be covered by the height of the patch. The geometric structure of the patch forces a squared configuration, then we discerned that by using $s = s_x = s_y = 3$ and $\gamma = 4$, the local patch and the descriptor can identify events of $9 \mu V$ of amplitude, with a span of $\lambda = 0.56$ seconds. This also determines that 1 pixel represents $\frac{1}{\gamma} = \frac{1}{4}\mu V$ on the vertical direction and $\frac{1}{F_s \gamma} = \frac{1}{64}$ seconds on the horizontal direction. The keypoints p_k are located at $(x_{p_k}, y_{p_k}) = (0.55F_s \gamma, z^l(c)) = (35, z^l(c))$ for the corresponding channel c and location l (see Equation 4). In this way the whole transient event is captured. Figure 4 shows a patch of a signal plot covering the complete amplitude (vertical direction) and the complete span of the signal event (horizontal direction).

Lastly, the number of channels C is equal to 8 for both datasets, and the number of intensification sequences k_a is fixed to 10. The parameter k used to construct the set $N_T(\mathbf{d}^{(l,c)})$ is assigned to $k = 7$, which was found empirically to achieve better results. In addition, the norm used on Equations 8 and 9 is the cosine norm, and descriptors are normalized to $[-1, 1]$.

3 RESULTS

Table 1 shows the results of applying the [proposed Histogram of Gradient Orientations \(HIST\)](#) algorithm to the subjects of the public dataset of ALS patients. The percentage of correctly spelled letters is calculated while performing an offline BCI Simulation. From the seven words for each subject, the first three are used for calibration, and the remaining four are used for testing. The best performing channel bpc is informed as well. The target ratio is 1 : 36; hence [theoretical](#) chance level is 2.8%. It can be observed that the best performance of the letter identification method is reached in a dissimilar channel depending on the subject being studied. This table shows for comparison the obtained performance rates using single-channel signals with the [SVM Support Vector Machine \(SVM\)](#) (?) classifier. This method is configured to use a linear kernel. The best performing channel, where the best letter identification rate was achieved, is also depicted.

The Information Transfer Rate (ITR), or Bit Transfer Rate (BTR), in the case of reactive BCIs (?) depends on the amount of signal averaging required to transmit a valid and robust selection. Figure 5 shows the performance curves for varying intensification sequences for the subjects included in the dataset of ALS patients. It can be noticed that the percentage of correctly identified letters depends on the number of intensification sequences that are used to obtain the averaged signal. Moreover, when the number of intensification sequences tend to 1, which corresponds to single-intensification character recognition, the performance is reduced. As mentioned before, the SNR of the P300 obtained from only one segment of the intensification sequence is very low and the shape of its P300 component is not very well defined.

In Table 2 the results obtained for 8 healthy subjects are shown. It can be observed that the performance is above chance level [and higher than those achieved by the other method](#). [It was verified that HIST method has an improved performance at letter identification than SVM that process the signals on a channel by channel strategy \(Wilcoxon signed-rank test, \$p = 0.004\$ for both datasets\)](#).

Tables 3 and 4 are presented in order to compare the performance of the [Histogram of Gradient Orientations \(HIST\)](#) [HIST](#) method versus a multichannel version of the [SWLDA Stepwise Linear Discriminant Analysis \(SWLDA\)](#) and SVM classification algorithms for both datasets. The feature was formed by concatenating all the channels (?). SWLDA is the methodology proposed by the ALS dataset's publisher. Since authors ? did not report the Character Recognition Rate obtained for this dataset, we replicate their procedure and include the performance obtained with the SWLDA algorithm at letter identification. It was verified [that HIST method has an improved performance at letter identification than](#)

307 other methods that process the signals on a channel by channel strategy, and it even has a comparable
308 for the dataset of ALS patients that it has similar performance against other methods like SWLDA or
309 SVM, which uses use a multichannel feature (Quade test with $p = 0.55$) whereas for the dataset of healthy
310 subjects significant differences where found (Quade test with $p = 0.02$) where only the HIST method
311 achieved a different performance than SVM (with multiple comparisons, significant difference of level
312 0.05).

313 The P300 ERP consists of two overlapping components: the P3a and P3b, the former with frontocentral
314 distribution while the later stronger on centroparietal region (?). Hence, the standard practice is to find
315 the stronger response on the central channel Cz (?). However, ? show that the response may also arise in
316 occipital regions. We found that by analyzing only the waveforms, occipital channels PO8 and PO7 show
317 higher performances for some subjects.

318 As subjects have varying *latencies* and *amplitudes* of their P300 components, they also have a varying
319 stability of the *shape* of the generated ERP (?). Figure 6 shows 10 sample P300 templates patches for
320 patients 8 and 3 from the dataset of ALS patients. It can be discerned that in coincidence with the
321 performance results, the P300 signature is more clear and consistent for subject 8 (A) while for subject 3
322 (B) the characteristic pattern is more difficult to perceive.

323 Additionally, the stability of the P300 component waveform has been extensively studied in patients
324 with ALS (?????) where it was found that these patients have a stable P300 component, which were also
325 sustained across different sessions. In line with these results we do not find evidence of a difference in
326 terms of the performance obtained by analyzing the waveforms (HIST) for the group of patients with ALS
327 and the healthy group of volunteers (Mann-Whitney U Test, $p = 0.46$). Particularly, the best performance
328 is obtained for a subject from the ALS dataset for which, based on visual observation, the shape of they
329 P300 component is consistently identified.

330 It is important to remark that when applied to binary images obtained from signal plots, the feature
331 extraction method described in Section 2.1.3 generates sparse descriptors. Under this subspace we found
332 that using the cosine metric yielded a significant performance improvement. On the other hand, the unary
333 classification scheme based on the NBNN algorithm proved very beneficial for the P300 Speller Matrix.
334 This is due to the fact that this approach solves the unbalance dataset problem which is inherent to the
335 oddball paradigm (?).

4 DISCUSSION

336 Among other applications of Brain Computer Interfaces, the goal of the discipline is to provide
337 communication assistance to people affected by neuro-degenerative diseases, who are the most likely
338 population to benefit from BCI systems and EEG processing and analysis.

339 In this work, a method to detect transient P300 components from EEG signals based on their waveform
340 characterization in digital time-space, extract an objective metric from the waveform of the plots of EEG
341 signals is presented. Its usage to implement a valid P300-Based BCI Speller application is expounded.
342 Additionally, its validity is evaluated using a public dataset of ALS patients and an own dataset of healthy
343 subjects.

344 It was verified that this method has an improved performance at letter identification than other methods
345 that process the signals on a channel by channel strategy, and it even has a comparable performance against
346 other methods like SWLDA or SVM, which uses a multichannel feature. Furthermore, this method has the

347 advantage that shapes of waveforms can be analyzed in an objective way. We observed that the shape of
348 the P300 component is more stable in occipital channels, where the performance for identifying letters
349 is higher. We additionally verified that ALS P300 signatures are stable in comparison to those of healthy
350 subjects.

351 We believe that the use of descriptors based on histogram of gradient orientation, presented in this work,
352 can also be utilized for deriving a shape metric in the space of the P300 signals which can complement
353 other metrics based on time-domain as those defined by ?. It is important to notice that the analysis of
354 waveform shapes is usually performed in a qualitative approach based on visual inspection (?), and a
355 complementary methodology which offer a quantitative metric will be beneficial to these routinely analysis
356 of the waveform of ERPs.

357 The goal of this work is to answer the question if a P300 component could be solely determined by
358 inspecting automatically their waveforms. We conclude affirmatively, though two very important issues
359 still remain:

360 First, the stability of the P300 in terms of its shape is crucial: the averaging procedure, montages, the
361 signal to noise ratio and spatial filters all of them are non-physiological factors that affect the stability of
362 the shape of the P300 ERP. We tested a preliminary approach to assess if the morphological shape of the
363 P300 of the averaged signal can be stabilized by applying different alignments of the stacked segments (see
364 Figure 2) and we verified that there is a better performance when a correct segment alignment is applied.
365 We applied Dynamic Time Warping (DTW) (?) to automate the alignment procedure but we were unable
366 to find a substantial improvement. Further work to study the stability of the [shape of the](#) P300 signature
367 component needs to be addressed.

368 The second problem is the amplitude variation of the P300. We propose a solution by standardizing the
369 signal, shown in Equation 2. It has the effect of normalizing the peak-to-peak amplitude, moderating its
370 variation. It has also the advantage of reducing noise that was not reduced by the averaging procedure. It is
371 important to remark that the averaged signal variance depends on the number of segments used to compute
372 it (?). The standardizing process converts the signal to unit signal variance which makes it independent of
373 the number k_a of signals averaged. Although this is initially an advantageous approach, the standardizing
374 process reduces the amplitude of any significant P300 complex diminishing its automatic interpretation
375 capability.

376 In our opinion, the best benefit of the presented method is that a closer collaboration [of the field of](#)
377 [BCI](#) with physicians can be fostered (?), since this procedure intent to imitate human visual observation.
378 Automatic classification of patterns in EEG that are specifically identified by their shapes like K-Complex,
379 Vertex Waves, Positive Occipital Sharp Transient (?) are a prospect future work to be considered. We are
380 currently working in unpublished material analyzing K-Complex components that could eventually provide
381 assistance to physicians to locate these EEG patterns, specially in long recording periods, frequent in sleep
382 research (?). Additionally, it can be used for artifact removal which is performed on many occasions by
383 visually inspecting signals. This is due to the fact that the descriptors are a direct representation of the shape
384 of signal waveforms. In line with these applications, it can be used to build a database (?) of quantitative
385 representations of waveforms and improve atlases (?), which are currently based on qualitative descriptions
386 of signal shapes.

CONFLICT OF INTEREST STATEMENT

387 The authors declare that the research was conducted in the absence of any commercial or financial
 388 relationships that could be construed as a potential conflict of interest.

AUTHOR CONTRIBUTIONS

389 This work is part of the PhD thesis of RR which is directed by JS and codirected by AV.

FUNDING

390 This project was supported by the ITBACyT-15 funding program issued by ITBA University from Buenos
 391 Aires, Argentina.

Table 1. Character recognition rates for the public dataset of ALS patients using the Histogram of Gradient (HIST) calculated from single-channel plots. Performance rates using single-channel signals with the SVM classifier are shown for comparison. The best performing channel *bpc* for each method is visualized

Participant		bpc	HIST	bpc	Single Channel SVM
1	Cz	35%	Cz		15%
2	Fz	85%	PO8		25%
3	Cz	25%	Fz		5%
4	PO8	55%	Oz		5%
5	PO7	40%	P3		25%
6	PO7	60%	PO8		20%
7	PO8	80%	Fz		30%
8	PO7	95%	PO7		85%

Table 2. Character recognition rates for the own dataset of healthy subjects using the Histogram of Gradient (HIST) calculated from single-channel plots. Performance rates using single-channel signals with the SVM classifier are shown for comparison. The best performing channel *bpc* for each method is visualized.

Participant		bpc	HIST	bpc	Single Channel SVM
1	Oz	40%	Cz		10%
2	PO7	30%	Cz		5%
3	P4	40%	P3		10%
4	P4	45%	P4		35%
5	P4	60%	P3		10%
6	Pz	50%	P4		25%
7	PO7	70%	P3		30%
8	P4	50%	PO7		10%

Table 3. Character recognition rates *and the best performing channel bpc* for the public dataset of ALS patients using the Histogram of Gradient (HIST) ~~calculated from plots of single channels with the best performing channel bpc informed as well~~(repeated here for comparison purposes). Performance rates obtained by SWLDA and SVM classification algorithms with a multichannel concatenated feature.

Participant	bpc for HIST	HIST	Multichannel SWLDA	Multichannel SVM
1	Cz	35%	45%	40%
2	Fz	85%	30%	50%
3	Cz	25%	65%	55%
4	PO8	55%	40%	50%
5	PO7	40%	35%	45%
6	PO7	60%	35%	70%
7	PO8	80%	60%	35%
8	PO7	95%	90%	95%

Table 4. Character recognition rates *and the best performing channel bpc* for the own dataset of healthy subjects using the Histogram of Gradient (HIST) ~~calculated from plots of single channels with the best performing channel bpc informed as well~~(repeated here for comparison purposes). Performance rates obtained by SWLDA and SVM classification algorithms with a multichannel concatenated feature.

Participant	bpc for HIST	HIST	Multichannel SWLDA	Multichannel SVM
1	Oz	40%	65%	40%
2	PO7	30%	15%	10%
3	P4	40%	50%	25%
4	P4	45%	40%	20%
5	P4	60%	30%	20%
6	Pz	50%	35%	30%
7	PO7	70%	25%	30%
8	P4	50%	35%	20%

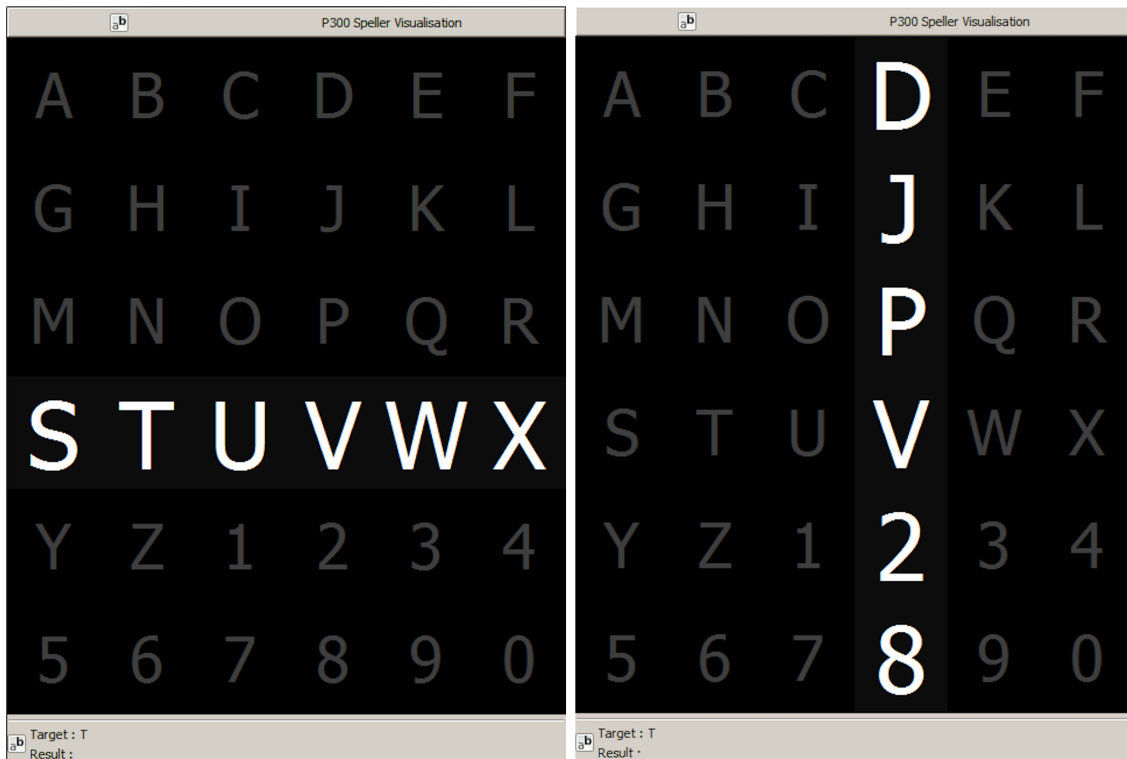


Figure 1. Example of the 6×6 Speller Matrix used in the study obtained from the OpenVibe software. Rows and columns flash in random permutations.

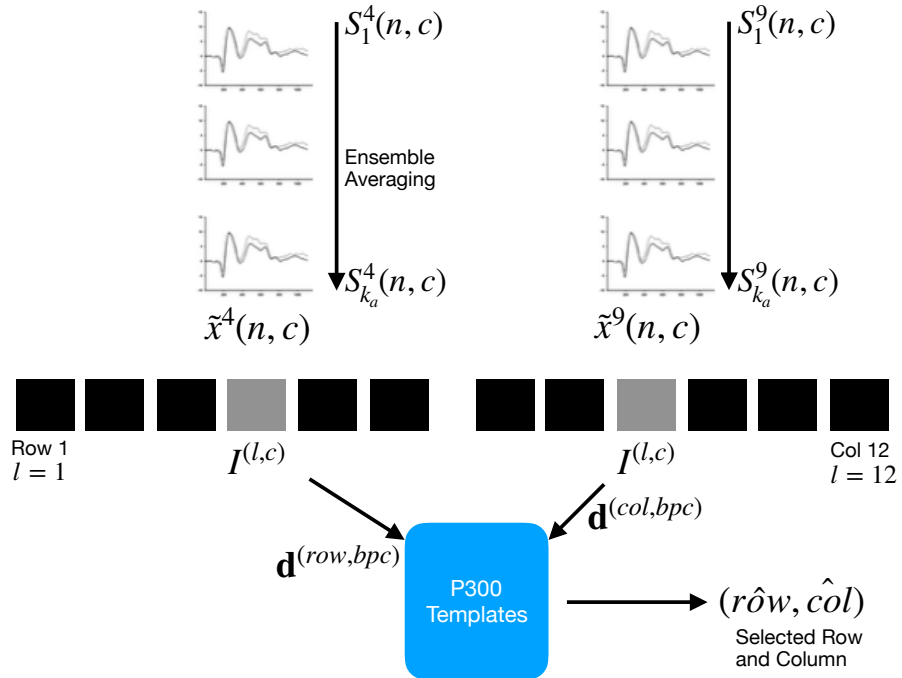


Figure 2. For each column and row, an averaged, standardized and scaled signal $\tilde{x}^l(n, c)$ is obtained from the segments S_i^l corresponding to the k_a intensification sequences with $1 \leq i \leq k_a$ and location l varying between 1 and 12. From the averaged signal, the image $I^{(l,c)}$ of the signal plot is generated and each descriptor is computed. By comparing each descriptor against the set of templates, the P300 ERP can be detected, and finally the desired letter from the matrix can be inferred.

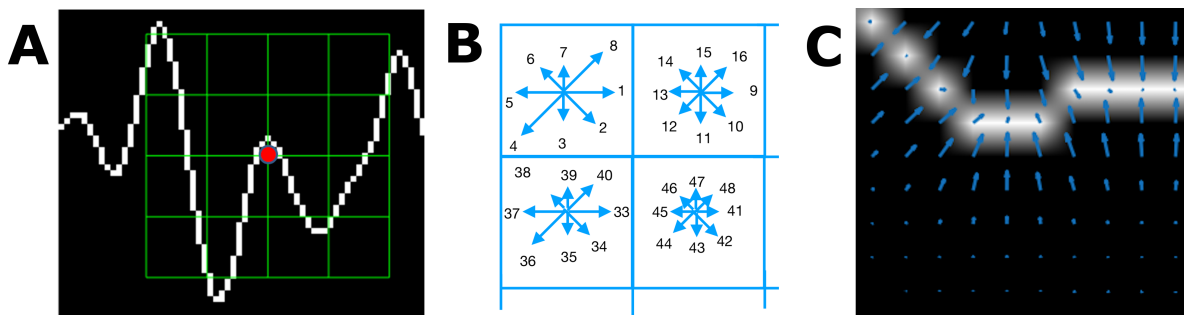


Figure 3. (A) Example of a plot of the signal, a keypoint and the corresponding patch. (B) A scheme of the orientation's histogram computation. Only the upper-left four blocks are visible. The first eight orientations of the first block, are labeled from 1 to 8 clockwise. The orientation of the second block $B_{1,2}$ is labeled from 9 to 16. This labeling continues left-to-right, up-down until the eight orientations for all the sixteen blocks are assigned. They form the corresponding descriptor of 128 coordinates. The length of each arrow represent the value of the histogram on each direction for each block. (C) Vector field of oriented gradients. Each pixel is assigned an orientation and magnitude calculated using finite differences.

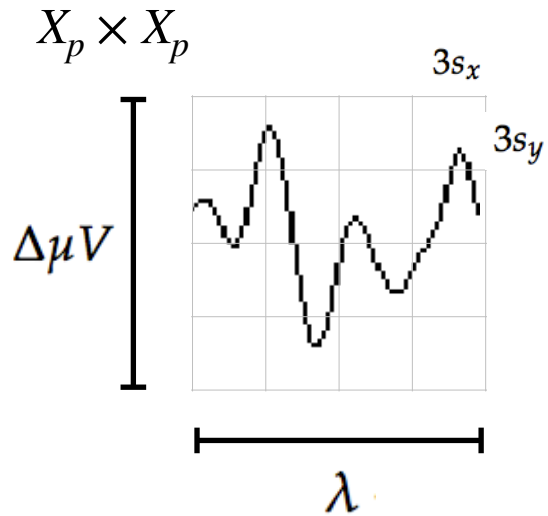


Figure 4. The scale of local patch is selected in order to capture the whole transient event. The size of the patch is $X_p \times X_p$ pixels. The vertical size consists of 4 blocks of size $3s_y$ pixels which is high enough as to contain the signal $\Delta\mu V$, the peak-to-peak amplitude of the transient event. The horizontal size includes 4 blocks of $3s_x$ and covers the entire duration in seconds of the transient signal event, λ .

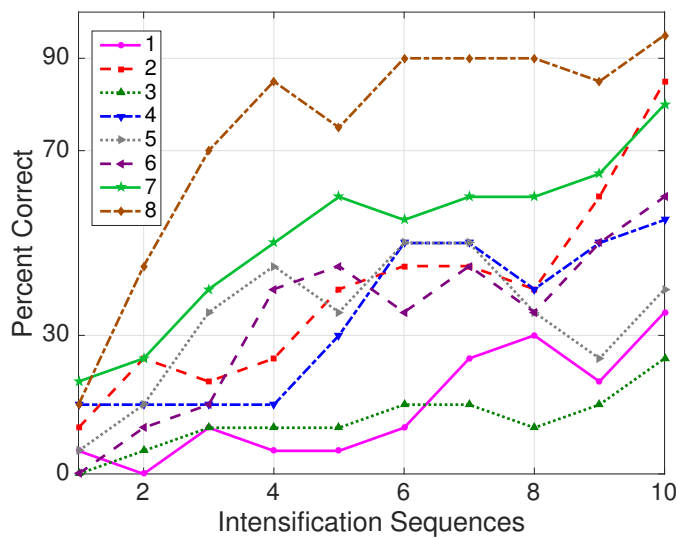


Figure 5. Performance curves for the eight subjects included in the dataset of ALS patients. Three out of eight subjects achieved the necessary performance to implement a valid P300 speller.

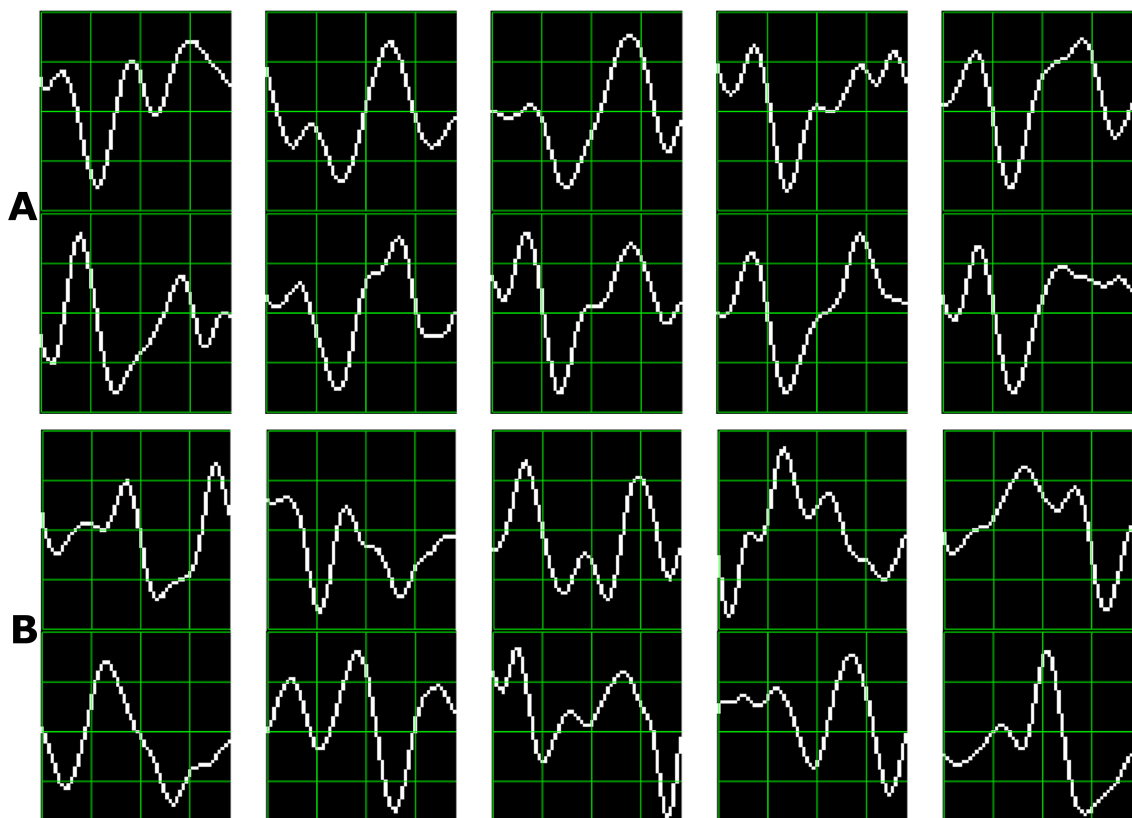


Figure 6. Ten sample P300 template patches for subjects 8 (A) and 3 (B) of the ALS Dataset. Downward deflection is positive polarity.